Review Article

Anatomic, functional and molecular imaging in lung cancer precision radiation therapy: treatment response assessment and radiation therapy personalization

Michael MacManus[1,2], Sarah Everitt[1,2], Tanja Schimek-Jasch[3], X. Allen Li[4], Ursula Nestle[3,5], Feng-Ming (Spring) Kong[6]

[1]Department of Radiation Oncology, Division of Radiation Oncology and Cancer Imaging, Peter MacCallum Cancer Centre, Melbourne, Australia; [2]The Sir Peter MacCallum Department of Oncology, The University of Melbourne, Parkville, Australia; [3]Department of Radiation Oncology, Medical Center, Faculty of Medicine, University of Freiburg, German Cancer Consortium (DKTK) Partner Site Freiburg, German Cancer Research Center (DKFZ), Heidelberg, Germany; [4]Department of Radiation Oncology, Medical College of Wisconsin, WI, USA; [5]Department of Radiation Oncology, Kliniken Maria Hilf, Moenchengladbach, Germany; [6]Indiana University Simon Cancer Center, Indiana University School of Medicine, Indianapolis, IN, USA

Contributions: (I) Conception and design: All authors; (II) Administrative support: None; (III) Provision of study materials or patients: All authors; (IV) Collection and assembly of data: All authors; (V) Data analysis and interpretation: All authors; (VI) Manuscript writing: All authors; (VII) Final approval of manuscript: All authors.

Correspondence to: Professor Michael MacManus. Department of Radiation Oncology, Peter MacCallum Cancer Centre, 305 Grattan Street, Melbourne, Vic 3000, Australia. Email: michael.macmanus@petermac.org.

Abstract: This article reviews key imaging modalities for lung cancer patients treated with radiation therapy (RT) and considers their actual or potential contributions to critical decision-making. An international group of researchers with expertise in imaging in lung cancer patients treated with RT considered the relevant literature on modalities, including computed tomography (CT), magnetic resonance imaging (MRI) and positron emission tomography (PET). These perspectives were coordinated to summarize the current status of imaging in lung cancer and flag developments with future implications. Although there are no useful randomized trials of different imaging modalities in lung cancer, multiple prospective studies indicate that management decisions are frequently impacted by the use of complementary imaging modalities, leading both to more appropriate treatments and better outcomes. This is especially true of ^{18}F-fluoro-deoxyglucose (FDG)-PET/CT which is widely accepted to be the standard imaging modality for staging of lung cancer patients, for selection for potentially curative RT and for treatment planning. PET is also more accurate than CT for predicting survival after RT. PET imaging during RT is also correlated with survival and makes response-adapted therapies possible. PET tracers other than FDG have potential for imaging important biological process in tumors, including hypoxia and proliferation. MRI has superior accuracy in soft tissue imaging and the MRI Linac is a rapidly developing technology with great potential for online monitoring and modification of treatment. The role of imaging in RT-treated lung cancer patients is evolving rapidly and will allow increasing personalization of therapy according to the biology of both the tumor and dose limiting normal tissues.

Keywords: Lung cancer; positron emission tomography (PET); magnetic resonance imaging (MRI); radiation therapy (RT)

Submitted Jul 27, 2017. Accepted for publication Sep 13, 2017.
doi: 10.21037/tlcr.2017.09.05
View this article at: http://dx.doi.org/10.21037/tlcr.2017.09.05

Introduction

The modern management of lung cancer with radiation therapy (RT) is critically dependent on imaging (1). Diagnosis, staging, patient selection, tumor and target volume (TV) definition, motion management and therapeutic response assessment all rely heavily on an accurate delineation of the tumor and its anatomic environment. As highlighted in other articles in this issue, advances in imaging have contributed to the improved outcomes observed in lung cancer reported in recent years and new imaging modalities are becoming available with the potential to further advance the field. Rapid developments in imaging have benefited patients by increasing the accuracy of three- and four-dimensional delineation of their disease, with computed tomography (CT), magnetic resonance imaging (MRI) and most recently by positron emission tomography (PET), especially when ^{18}F-fluoro-deoxyglucose (FDG)-PET is combined with CT in PET/CT images. Furthermore by providing information concerning molecular or functional characteristics of tumors, it will be possible to use factors such as tumor glucose uptake, perfusion, hypoxia and proliferation to help estimate prognosis and even select systemic therapies for use in combination with radiation. In an era of increasing personalization of treatment based on tumor biology, molecularly targeted therapies such as epidermal growth factor receptor tyrosine kinase inhibitors (EGFR TKIs) (2) and anatomically-targeted therapies such as stereotactic ablative radiation therapy (SABR) (3) are becoming more common. Imaging provides essential information that underpins the increasingly complex therapeutic decision making processes in the current management of lung cancer. Each imaging modality has its own strengths and limitations and a combination of one or more of these in multi-modality imaging is becoming increasingly common in the management of lung cancer. This review article aims to discuss the role of imaging in precision radiotherapy.

Imaging for precision decision making in radiotherapy

The aim of curative-intent precision RT in lung cancer is to control all sites of gross disease by the delivery of an anatomically targeted radiation dose sufficient to cause the eventual death of all clonogenic tumor cells with the least possible toxicity due to unnecessary irradiation of normal tissues. For the delivery of targeted RT to be successful, a great deal of information must be available about the tumor, including its precise anatomical location, its relation to normal tissues, its boundaries, the extent to which it is locally invasive, how it moves with respiration and cardiac motion, the extent and precise location of involved regional nodes and the number and location of any distant metastases that may be present. This information is obtained predominantly from imaging, although supplemented when appropriate by the results of biopsies, including endoscopic bronchoscopic ultrasound-guided biopsy EBUS (4), and other information such as operation notes for patients who have undergone surgical procedures.

The scope of radical or potentially curative RT in lung cancer has gradually expanded to include the curative-intent treatment of patients with intracranial oligometastasis with stereotactic radiosurgery and those with extracranial oligometastasis (5,6) who are treated with SABR. A more recent development is the use of targeted RT in patients with advanced non-small cell lung cancer (NSCLC) who have experienced responses to systemic therapies with chemotherapy or targeted therapies. In a recent randomized trial, Gomez and colleagues reported improved progression free survival (PFS) in patients with oligometastatic NSCLC without progression after first-line systemic therapy who received local radiotherapy compared to those who received no further treatment (7). Selective targeting of oligoprogressive disease sites with SABR may extend the period during which a useful response to systemic therapy may be experienced, even though cure is not the ultimate aim. External beam RT is always accompanied by the delivery of significant doses of radiation to sites outside of the TV, some of which may contain occult tumor. Both inadvertently delivered radiation dose, absorbed outside the planning target volume (PTV), and treatment deliberately targeted to regions of suspected microscopic disease, as in elective nodal irradiation (ENI), could potentially contribute to locoregional tumor control (LRTC), although the latter may have little impact in the era of modern imaging (8). Other treatment related factors that may contribute to long-term disease control, include concomitantly delivered platinum based chemotherapy and, potentially, changes in immunity generated by therapy (9).

All therapeutic approaches with RT in lung cancer, from curative treatment of stage IA tumours with SABR to radical chemoradiation in stage IIIB disease depend absolutely on three-, and four-dimensional imaging to accurately

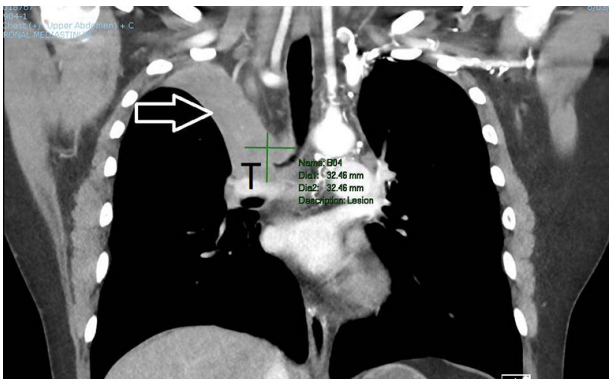

Figure 1 Value of CT in local assessment of lung cancer. Detailed information obtained in a lung cancer patient from contrast-enhanced CT. This patient has a right hilar NSCLC (T), which has caused thrombosis of the superior vena cava and brachiocephalic vein (arrow) and is associated with extensive collateral vessel dilatation. CT, computed tomography; NSCLC, non-small cell lung cancer.

characterize potentially malignant lesions. It is often impractical or impossible to biopsy every suspected lesion in a patient with locoregionally advanced lung cancer and therefore imaging characteristics must be used to determine the nature of individual lymph nodes or pulmonary nodules, to define them as benign or malignant and to decide if they should be included within the RT TV. In this regard, anatomical imaging is often insufficient by itself for accurate characterization and the addition of molecular imaging, primarily with FDG-PET, is required for the most accurate assessment of true disease status.

Imaging for precision staging or pre-treatment assessment for radiotherapy

Staging information is essential for determining treatment choice after a diagnosis of lung cancer. It is the primary factor for categorizing patients as potentially curable with surgery, RT or chemoradiation or having incurable disease that should be managed with palliative approaches intended to relieve symptoms and extend high quality survival time. Although CT scanning has been the standard 3-dimensional imaging tool for staging lung cancer, it has relatively poor ability to distinguish different structures in the soft-tissue density range and to distinguish tumor from surrounding soft tissue. The accuracy of CT in this regard is enhanced by co-registration with metabolic information derived from FDG-PET scanning, as discussed below. CT can provide invaluable clinical information on other relevant disease processes such as presence of thrombi in major vascular structures (*Figure 1*). FDG-PET and FDG-PET/CT can improve staging accuracy of locoregional and distant disease by 10–30% depending on initial apparent stage.

Because of its superb ability to provide detailed images of soft tissues, MRI scanning may often be complementary to CT. CT has more robust spatial accuracy and excellent capacity to image bone. A further capacity of MRI is the ability of functional MRI to derive additional information concerning biological processes occurring within the body. This biological information may eventually have wide application in oncology although the field is at an early stage of development.

Anatomic staging with CT and MRI

The staging system for lung cancer has gradually evolved into a powerful tool for standardized documentation of disease extent, prognostic stratification and selection of appropriate therapy. The most recent iteration of the system has made further refinements including revisions of the criteria for defining T stage in relation to potential resectability and sub-classifying metastatic disease according to number and location of lesions (10). The abilities of imaging studies to demarcate tumor margins by defining limits of invasion into adjacent normal tissues, to assign the true status of involvement of regional lymph nodes and detect distant metastasis are central in determining the true TNM status of the patient and guiding management along the most appropriate pathway.

The anatomic criteria for assigning lymph node stage are similar for CT and MRI imaging and relate entirely to the physical dimensions of the nodes (11). The most widely adopted convention for classifying lymph nodes using anatomic imaging is to consider nodes with short axis transverse diameter >1 cm to be positive. This approach leads to frequent false negatives and false positives because enlarged reactive nodes are common, as are normal sized nodes containing tumor. A recent attempt to derive additional information on nodal status from CT scans involved the use of texture analysis and reported improved accuracy with this approach (12).

CT is the workhorse for anatomic staging of lung cancer

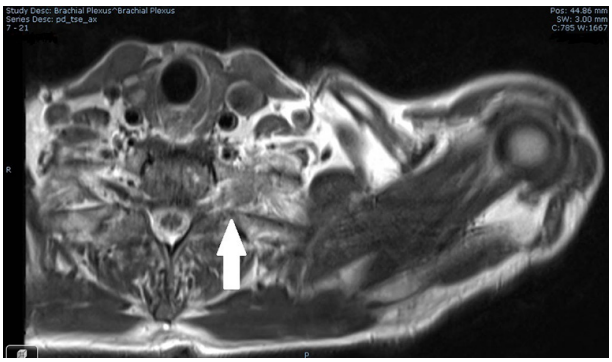

Figure 2 Detection of nerve root infiltration by MRI. MRI scan showing invasion of the T1 nerve root by a left sided apical lung cancer (arrow). This was not visualized on contemporaneous CT imaging. MRI, magnetic resonance imaging, CT, computed tomography.

for RT. It is capable of accurately delineating accurately lymph node size. It is an excellent high resolution modality for measuring dimensions of lung tumors that are entirely surrounded by aerated lung. It can account for movement and can be repeated during treatment for quality control, although the resolution of Cone Beam CT (CBCT) is poor, especially in large patients. CT is often inaccurate in determining the margins of tumors that are in contact with atelectatic lung and for defining the extent of tumor invasion into contiguous soft tissues with similar CT-density to tumor. This is especially the case for superior sulcus tumors with invasion into the brachial plexus where it is critical to define tumor margins accurately (*Figure 2*). In these settings MRI scanning can provide accurate information on local tumor invasion and these images can be fused with the corresponding CT images for use in RT planning (13).

For anatomical staging of suspected metastases CT and MRI may be complementary, as in the case of the adrenal gland, where MRI can help distinguish between CT-detected adrenal enlargement due to benign adenoma or hyperplasia from metastatic lung cancer. However, the addition of FDG-PET information to anatomic with CT and/or MRI greatly increases the accuracy of assessment of adrenal lesions (14). For staging of the brain in lung cancer, MRI is clearly superior to CT with much greater sensitivity and both CT and MRI are superior to FDG-PET for the detection of small brain metastases (15,16). However, despite the well documented strengths of anatomical imaging with CT and MRI, some significant weaknesses exist which may be overcome by adding functional imaging to the staging paradigm. These weaknesses include poor ability to distinguish benign from malignant lymph nodes in the thorax and inefficiency in the detection of extracranial distant metastasis.

Baseline evaluation of normal tissues

Lung cancer patients often have ventilation and perfusion defects related to lung disease and to thromboembolism. Ventilation and perfusion (V/Q) scans are sometimes used to determine if a patient is suitable for surgical resection and can provide information that is valuable for distinguishing high functioning from low functioning lung. V/Q SPECT data indicate that ventilation and perfusion defects are greater in central then in peripheral tumors (17). Moreover, apparently normal areas of lung on CT often have impaired function as measured by V/Q SPECT (18). Importantly, regional ventilation and perfusion may improve during RT for centrally located NSCLC (18). More recently, V/Q imaging with PET tracers has become available. For example, ^{68}Ga-VQ respiratory gated (4-D) PET/CT scans (19) provide much higher resolution and accuracy than SPECT and may have potential in radiotherapy planning by allowing high functioning lung to be spared and for dose to be "dumped " in areas of lung with poor perfusion and / or ventilation (20)

Molecular staging with PET and PET/CT

Characterizing the primary tumor

As discussed above, purely anatomical imaging of lung cancer with CT or MRI has limitations in the staging of lung cancer. Evaluation of the local extent of lung cancer is especially problematic in the presence of significant atelectasis because the soft tissue densities of pulmonary and tumor tissue may be similar and tumor margins inapparent. FDG-PET can help distinguish the boundary between tumor and atelectatic lung. Locally advanced lung cancers are often associated with nodules in nearby lung which could represent benign processes or may alternatively be satellite nodules, intrapulmonary nodal metastases or haematogenous metastases. It is known from the PET literature on the evaluation of solitary pulmonary nodules (SPNs) that strongly FDG-avid lesions are very likely to be

malignant (21) in the absence of an alternative explanation such as mycobacterial or fungal infection. When biopsy is not performed, PET information is extremely valuable when making decisions about the nature of additional pulmonary nodules in patients with locoregionally advanced lung cancers. Patients with undiagnosed SPNs that are suspicious for lung cancer on structural imaging may have serious comorbidities, including severe emphysema with bullae, which preclude both a safe attempt at needle biopsy and any chance of a curative surgical resection. In such cases demonstration of high FDG uptake on PET can be used as a surrogate for biopsy and allow the patient to proceed to curative intent treatment with SABR or conventional RT.

Mediastinal nodal staging

In routine practice, a short axis length of 1 cm is taken as the cut-off for involvement by tumor of intrathoracic nodes. Unfortunately, smaller nodes may still contain tumor and large nodes may simply be reactive or enlarged due to entirely different pathology such as histoplasmosis or sarcoidosis. Use of a larger cut-off diameter would make the assessment more specific but less sensitive and vice versa. Multiple surgical series and several meta-analyses have confirmed the poor staging performance of CT as a single staging modality and shown that an assessment based on PET, especially when PET and CT are combined, can provide a much more accurate assessment of the true status of mediastinal nodes. In the meta-analysis of Gould and colleagues, FDG-PET was more accurate than CT for identifying lymph node involvement (P<0.001). For CT, median sensitivity and specificity were 61% and 79% respectively and for PET, median sensitivity and specificity were 85% and 90% respectively. FDG-PET was more sensitive but less specific when lymph nodes were enlarged (median sensitivity, 100% median specificity, 78% than when nodal size was normal (median sensitivity, 82%; median specificity, 93%; P=0.002). The use of fused PET/CT images provides the best non-invasive means for intrathoracic nodal staging and may be both more accurate and cost saving than non-PET approaches (22).

For evaluation of patients with NSCLC, PET/CT is best used in combination with selective use of nodal biopsy, such as at mediastinoscopy (23) or with EBUS (4,24), to clarify nodal status when key decisions are to be made concerning surgery or in determining which nodal stations need to be included in RT TVs.

Detection of distant extracranial metastasis

Patients with lung cancer have a very high risk of developing distant metastasis, especially those with locoregionally-advanced lesions in the thorax. One of the main goals of primary staging is to detect distant metastasis when present and to direct the patient towards the most appropriate form of therapy, whether palliative RT or systemic therapy in the setting of truly extensive metastatic disease, curative surgery or RT when disease is more localized, or towards SABR or other definitive therapies for patients with oligometastatic disease. Although CT scanning is useful in detecting pulmonary metastasis, it is less sensitive and specific than PET/CT at most extracranial sites including, liver, bone (*Figure 3A*) (25) and adrenal. The probability that PET imaging will detect unsuspected distant metastasis in patients previously staged with CT increases with increasing AJCC stage group. In a study of 167 patients with apparent stage I-III NSCLC, PET-detected metastasis increased with increasing pre-PET stage from I (7.5%) through II (18%) to III (24%, P=0.016), and, in particular, was significantly higher in Stage III (P=0.039) (26).

A significant limitation of FDG-PET in staging the brain is the high FDG background uptake of normal cerebral tissue. This is not a limitation for the experimental proliferation tracer ^{18}F-fluorothymidine (FLT), where cerebral uptake is low. FLT PET/CT detected unsuspected cranial metastases in 3 of 60 patients who were enrolled in prospective studies of proliferation imaging during RT (27).

Outcomes for PET-selected patients and timeliness of staging

The routine use of PET for staging and selection for treatment with RT has been shown to be associated with improved outcomes in patients with NSCLC (28), compared to non-PET staged cohorts. In a study of 153 patients candidates for curative intent RT, 46 patients (30%) who were excluded from curative intent RT after PET because of advanced local or distant disease much worse (P=0.02) survival, indicating that treatment decisions based on PET were appropriate (29). In a more recent study, using PET/CT, the disparity on survival between the 66% selected for curative therapy and the remainder who received palliative treatment was even greater (30). Overall survival for patients given chemoRT was 77.5% and 35.6% at 1 and 4 years, respectively and for patients treated palliatively was 16.3% and 4.1% at 1 and 4 years,

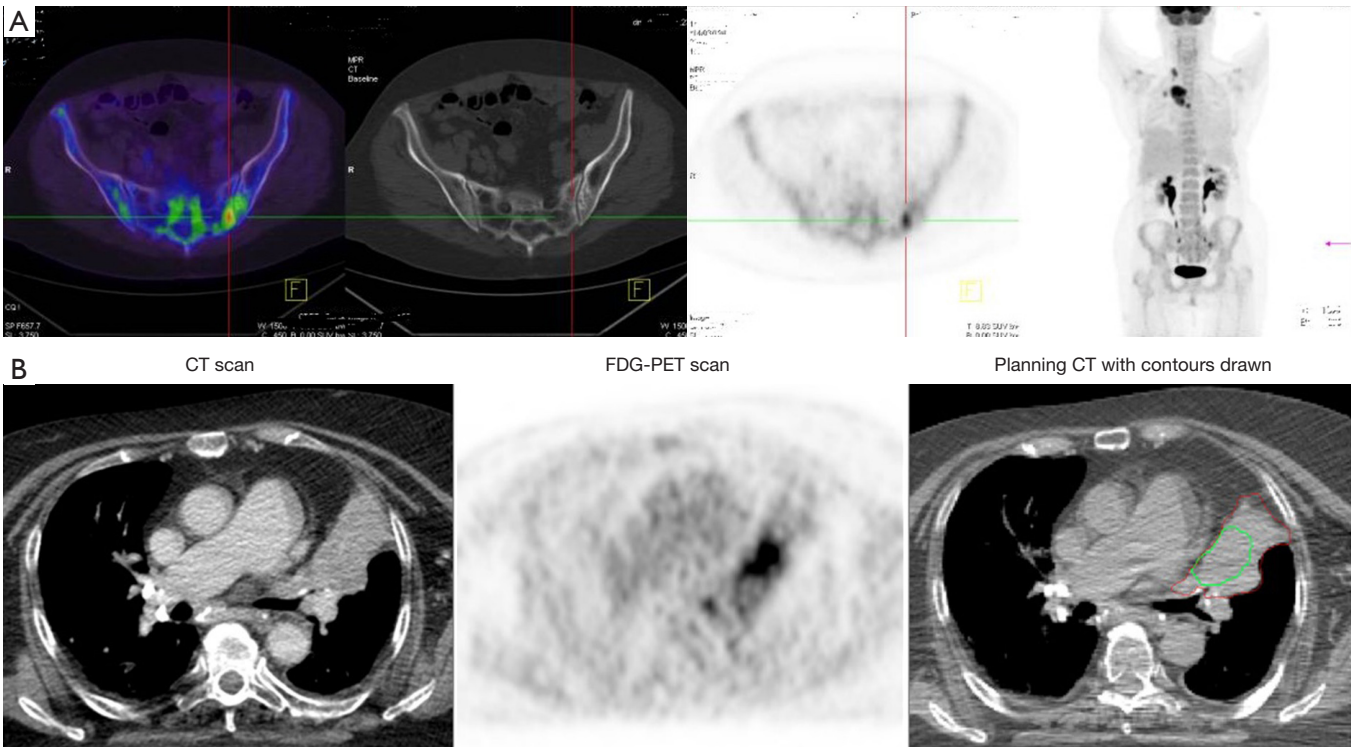

Figure 3 Incremental value of FDG-PET added to CT imaging. (A) FDG PET/CT scan of a patient with locoregionally advanced NSCLC being considered for curative intent RT. In addition to the known primary tumor and intrathoracic lymph node involvement, this scan showed unexpected distant bony metastases in the left sacrum (highlighted in cross hairs) and sternum; (B) this patient with stage IIIA NSCLC (SCC) of the left upper lobe was planned for combined chemo-RT. Atelectatic upper lobe was included in the GTV when CT was used for target delineation. When PET information was incorporated, tumor margins were clearly seen and a much smaller (green) GTV was contoured. FDG-PET, 18F-fluoro-deoxyglucose positron emission tomography; CT, computed tomography; NSCLC, non-small cell lung cancer; GTV, gross tumor volume.

respectively (P<0.001) (30).

It is important that PET staging for patients treated with RT should be timely because disease may progress rapidly in the interval between initial staging and treatment planning (31). Everitt and colleagues investigated the rate of tumor progression between staging and RT planning FDG-PET/CT scans in 28 patients. The median interscan period was 24 days and interscan disease progression (TNM stage) was detected in 11 (39%) patients. The probability of upstaging within 24 days was calculated to be 32% and treatment intent changed from curative to palliative in 8 (29%) cases, in 7 because of PET (32). Wang and colleagues also studied pre-treatment tumor progression and reported a 21% progression rate with a median inter-scan interval of 43 days (33). In a further study it was reported that patients who were denied curative RT progression between scans had an extremely poor prognosis (34). It was recommended in the 2015 International Atomic Energy Agency (IAEA) consensus report that the interval between staging PET and RT commencing should be no more than 3 weeks (35).

Use of imaging for RT planning and delivery

Imaging for TV delineation for radiotherapy

TV definition should incorporate all clinical and imaging information available. Usually, information on histology or cytology of the lung tumor and involved lymph nodes will be gathered by bronchoscopy including endoscopic esophageal ultrasound-guided fine needle aspiration (EUS-FNA), endoscopic endobronchial ultrasound-guided trans-bronchial needle aspiration (EBUS-TBNA), mediastinoscopy or CT-guided biopsy. The visualization of

the primary tumor and involved nodes as well as of normal tissue is usually based on a combination of multiple imaging methods including CT, FDG-PET/CT and sometimes MRI depending on tumor location and invasion.

Several uncertainties of anatomical imaging can be addressed by incorporating the FDG-PET information in the critical step of radiotherapy TV delineation, such as the discrimination of the gross tumor volume (GTV) of primary lesions from organs at risk, mediastinal structures or atelectasis (*Figure 3B*) (36). FDG-PET also facilitates the identification of involved mediastinal lymph nodes which need to be accounted for in the TV as discussed above (37).

PET imaging, and especially with the acquisition of a combined PET-CT in radiotherapy treatment position, has been shown to reduce intra- and inter-observer variation in TV delineation of lung tumors (38) . A range of methods used to include the PET information in the TV have been evaluated. Manual techniques, that is the visual interpretation and manual delineation of a PET based GTV (39), are widely-used. In recent years several auto-segmentation approaches have been reported to either guide or generate the TV (40). In spite of promising results, especially of algorithms based on more advanced image paradigms, the use of automatically generated PET contours for TV delineation without human visual and interdisciplinary interpretation of the images and verification of the GTV contour is not recommended (41,42). For visual assessment, standardized window/level settings are strongly suggested, since even marginal alterations can cause significant differences in the apparent tumor extent on PET images and thus in the resulting TV. The IAEA publication provides guidance on the use and role of PET-CT imaging for radiotherapy treatment planning in NSCLC (35). RTOG1106, a multicenter study requires PET metabolic tumor volumes to form the PTV at the baseline, using a combined method of autosegmentation thresholding at 1.5 ratio of mediastinum blood pool followed knowledge based manual editing (43).

As discussed above, MRI may additionally be useful for GTV delineation, especially in tumors invading the thoracic wall or the superior sulcus (including Pancoast tumors) (44) as well as for para-spinal tumors with suspected infiltration of the vertebrae and/or spinal cord (45). To allow for co-registered planning, MRI sequences should be acquired in the RT planning position. Alternatively, deformable image fusion may be considered.

4D CT is a standard imaging method for treatment planning in stereotactic body radiation therapy (SBRT) and in the modern era of 3D conformal RT or IMRT, as it can provide personalized margins accounting for target motion (46,47). For better tumor delineation, 3D PET scans can be combined with 4DCT. The impact of additional 4D PET information is promising but remains investigational and is under active investigation (48-50). Several translational research projects within prospective SBRT trials, such as the current Freiburg mono center phase II STRIPE trial or the European Organization for Research and Treatment of Cancer (EORTC) 2113-0813 Lungtech trial (51,52) address the roles of 3D and 4D PET-CT for pre-treatment staging, TV delineation, response evaluation and detection of local recurrence after SBRT.

Radiotherapy treatment planning of locally advanced NSCLC in a curative setting is based on TV delineation of all discernible tumor sites, usually consisting of the primary tumor and all involved lymph nodes. The restriction of TVs to the FDG-positive areas is supported by data from the 3D-CRT-era (53). However, potential benefits of this approach versus conventional RT planning, such as the possibility of dose escalation, a reduction of treatment associated side effects and the utilization of different IMRT techniques have not been examined in depth. Following a successful pilot trial (54), these questions are currently being investigated in the prospective randomized multi-center PET-Plan trial. Interestingly, within this trial, data from a blinded expert review demonstrated a significant inter-observer variability in the reporting of involved mediastinal lymph nodes, which—after a structured interventional harmonization process—could be reduced (55). These data underline the necessity for a standardized assessment of FDG PET-CT imaging used for radiotherapy treatment planning.

Beyond the "mere" detection of tumor tissue, FDG-PET based dose-painting and FDG-uptake intensity based escalation is a concept that has been investigated in the Netherlands PET boost trial (56). Dose escalation in hypoxic sub-volumes has also been demonstrated feasible (57). Further trials are required to discover if this approach can lead to improvements in survival and/or local disease control.

Anatomical/structural imaging during radiotherapy

Anatomical images commonly acquired during standard radiotherapy include those from image guided RT (IGRT)

using in-room imagers such as on board CBCT or in-room CT (CT on rails). CT or MRI scans acquired outside of the treatment room may also be used for treatment response assessment. The MRI-Linac offers very exciting potential for synchronous imaging and treatment but remains investigational as the technology evolves (58). CBCT is commonly and frequently obtained for difficult cases with TVs close to critical structures to ensure a high precision in patient positioning and limit clinical target volume (CTV) to PTV expansions. Thus, CBCT is widely available, is performed routinely in clinical practice and is usable for adaptive RT. CBCT image quality, however, compares extremely unfavorably with image quality of CT on rail, CT simulators or diagnostic CT scans. The lower image quality potentially could have a negative impact on the accuracy of RT response assessment and target and OAR delineation. CT on rails has the advantage of providing diagnostic quality images for patient positioning and they are also available for ART. At most centers a new planning CT scan is acquired for ART. Disadvantages of the approach include the need for additional imaging, associated time commitment from patients and the health care team, as well as significant associated costs.

The ability of CBCT and CT on rails to image the GTV size and location both inter- and/or intra-fractionally enables an assessment of patient position, organ movement due to respiration, tumor regression or progression, and lung deformation due to collapse or re-expansion (59). Michienzi and colleagues validated the accuracy of 3D CBCT for monitoring primary NSCLC during RT by comparing GTVs on CBCT to those on time-matched diagnostic CT during the first, second and fourth weeks of RT (60). In this study of 30 consecutive patients, comparable image quality and tumor volumes were observed between CBCT and diagnostic CT, although differences were observed in tumor location, especially in lower lobe tumors and larger patients. Compared to Michienzi and colleagues who observed GTV's were 10.8% larger on CBCT than on baseline CT, Atorjai and colleagues reported considerably larger average CBCT contours of 30%, when compared to CT in 12 NSCLC patients receiving stereotactic RT. These findings suggest that the slow acquisition time of conventional (3D) CBCT may be such a significant limitation that four-dimensional (4D) CBCT, may be required, especially for lower lobe tumors.

CBCT has also been utilized to monitor volumetric changes in tumors over the course of a treatment course, with regression rates of between 0.6–1.5% per fraction reported (60-63). The significance of volumetric regression, according to anatomical imaging methods alone, in terms of patient survival has not been established. In fact Koo and colleagues reported that the most rapid reductions in volume detected on CT imaging one month after completion of chemoradiation for stage III NSCLC were associated with worse overall survival (64). Despite its limitations, including relative poor image quality, the readily accessible nature of CBCT during treatment provides a powerful tool for prompting re-scanning with PET/CT should dose or volumetric adaptations be considered necessary. In addition to all above benefits of CBCT, CTs acquired with CT on rails may be used to assess radiation-induced effects on tumor and lung tissue during radiotherapy. A recent study reported that changes in quantitative features of the daily CTs acquired during radiotherapy were associated with treatment outcome (65). More prospective and retrospective studies are needed to support that such quantitative features from CT scans acquired during radiotherapy may be an effective imaging biomarker for early response assessment and, thus, for guiding ART.

Small cell lung cancer (SCLC) has been less well-studied than NSCLC but significant reductions in tumor volume are often observed on CT before the end of RT. In limited stage SCLC a median CT-based volume reduction of approximately 70% can be expected before the completion of concurrent chemoRT (66). Limited stage SCLC patients with greater tumor volume reduction (i.e., >45%) appear to have better locoregional control and longer overall survival than those with less volume reduction (66).

Response assessment with PET during RT

Response assessment with FDG-PET is superior to CT for predicting overall survival after chemoRT in NSCLC (67). Furthermore, during fractionated RT, FDG-PET/CT metabolic tumor responses occur more rapidly than responses assessed using CT and interim PET scans may be the most useful imaging modality if response-adapted therapy is intended. Sequential scans may be directly compared with an appropriately performed baseline study (68-71).

Slowly responding tumor regions typically receive higher

doses when a response-adapted treatment plan is created. In one study, when CT and FDG-PET were compared after two thirds of treatment had been completed, a reduction in metabolic tumor volume of 70% was observed while GTV assessed by CT was reduced only by 41% (P<0.001) (43). Metabolic tumor volume reduction was more pronounced after two thirds of a 3D conformal RT course (73% reduction) in comparison to a SBRT course (15% reduction).

Kong and colleagues reported that FDG-PET/CT response after approximately 45 Gy was associated with the ultimate post-treatment response to chemoradiation (72). The mean peak tumor FDG activity was 5.2 (95% CI, 4.0 to 6.4), 2.5 (95% CI, 2.0 to 3.0), and 1.7 (95% CI, 1.3 to 2.0) on pre-, during-, and post-RT scans, respectively, and the peak tumor activity during RT correlated strongly with the peak FDG activity 3 months after completion of RT (72). Interestingly, normalized (to aortic arch) max SUV was lowest in this small study of 15 patients, who were without evidence of disease, and highest in patients who succumbed to their disease (72). A poor response on during-RT FDG-PET imaging also has been reported to be associated with inferior PFS for patients receiving hypofractionated RT to 60–66 Gy in 3 Gy fractions (73). Importantly, there may be a correlation between radiation dose delivered and max SUV at that time with higher max SUV declines with higher radiation doses (74).

The optimum timing of response assessment for survival estimation and response-adapted therapy during RT is unknown. Very early imaging may be uninformative and very late scanning may not allow sufficient time for response-adapted therapy. In one cohort, there was significant intra- and inter-individual heterogeneity in the evolution of tumor SUV_{max} at early time points at 7 and 14 days after RT start (75).

Although ^{18}F-FDG is highly specific and sensitive for imaging tumors at baseline, its specificity may be reduced in the presence of ^{18}F-FDG-avid radiation-induced inflammation, thereby reducing reliability of metabolic response assessment in the tumor when scans are acquired during treatment (76,77). To overcome this limitation, exploratory studies of interim tumor response monitoring have focused on other hallmarks of cancer, including rapid cellular proliferation (e.g., FLT) and hypoxia (e.g., FMISO). The ability of FLT to detect an early proliferative response in NSCLC was reported by Everitt and colleagues who performed both FDG and FLT PET/CT scans during the second and fourth weeks of CRT in 60 patients (*Figure 4A*) (78). Recent findings of this study revealed that patients with tumors displaying stable disease (SD) on week two FLT PET/CT scans experienced significantly longer progression free and overall survival than patients with tumors that displayed a partial or complete reduction in FLT uptake (27). These results require confirmation in larger studies.

In addition to tumor metabolism and proliferation, hypoxia is a third hallmark of cancer that is common in NSCLC and can also be visualized with PET imaging (79). Both ^{18}F-misonadazole (F-MISO) and ^{18}F-fluoroazomycin arabinoside (FAZA) (80) have been used for clinical hypoxia imaging. Low tumor oxygen concentrations occur both due to the increased metabolic demands of rapidly proliferating metabolically dysregulated tumor cells and inadequate tumor vasculature. Hypoxia is associated with resistance to chemotherapy and RT and with increased metastases, which contribute to poor tumor control and patient survival. Identifying intra-tumoral regions of hypoxia could potentially lead to dose escalation of resistant hypoxic sub-volumes, especially with the availability of 4D imaging (80). Vera and colleagues acquired F-MISO, FDG and FLT PET/CT scans in five patients prior to and after approximately 46 Gy of RT. F-MISO uptake remained stable over this time, in contrast to FDG and FLT, which both decreased (81). Significant variations in baseline and intra-treatment hypoxia burden were observed in seven patients with stage III NSCLC who received up to four serial F-MISO PET scans acquired before, during and after RT alone (82). Trinkaus and colleagues reported that hypoxic tumor regions detected on FAZA-PET eventually become undetectable after successful RT (83).

Image-guided adaptive treatment

Adaptive RT was initially introduced in an effort to take account of setup errors and intrafraction motion (84-86) but opened the door to adaptation of therapy based on treatment response. Several groups are exploring PET/CT tumor response assessment during RT with the goal to adapt RT at around week 4 of a 6-week treatment course (*Figure 4B*). Other time points might be better for assessing organs at risk when the aim is to predict and ultimately limit toxicity. In a pilot study Feng and colleagues reported that replanning based on during-RT PET/CT allowed for a

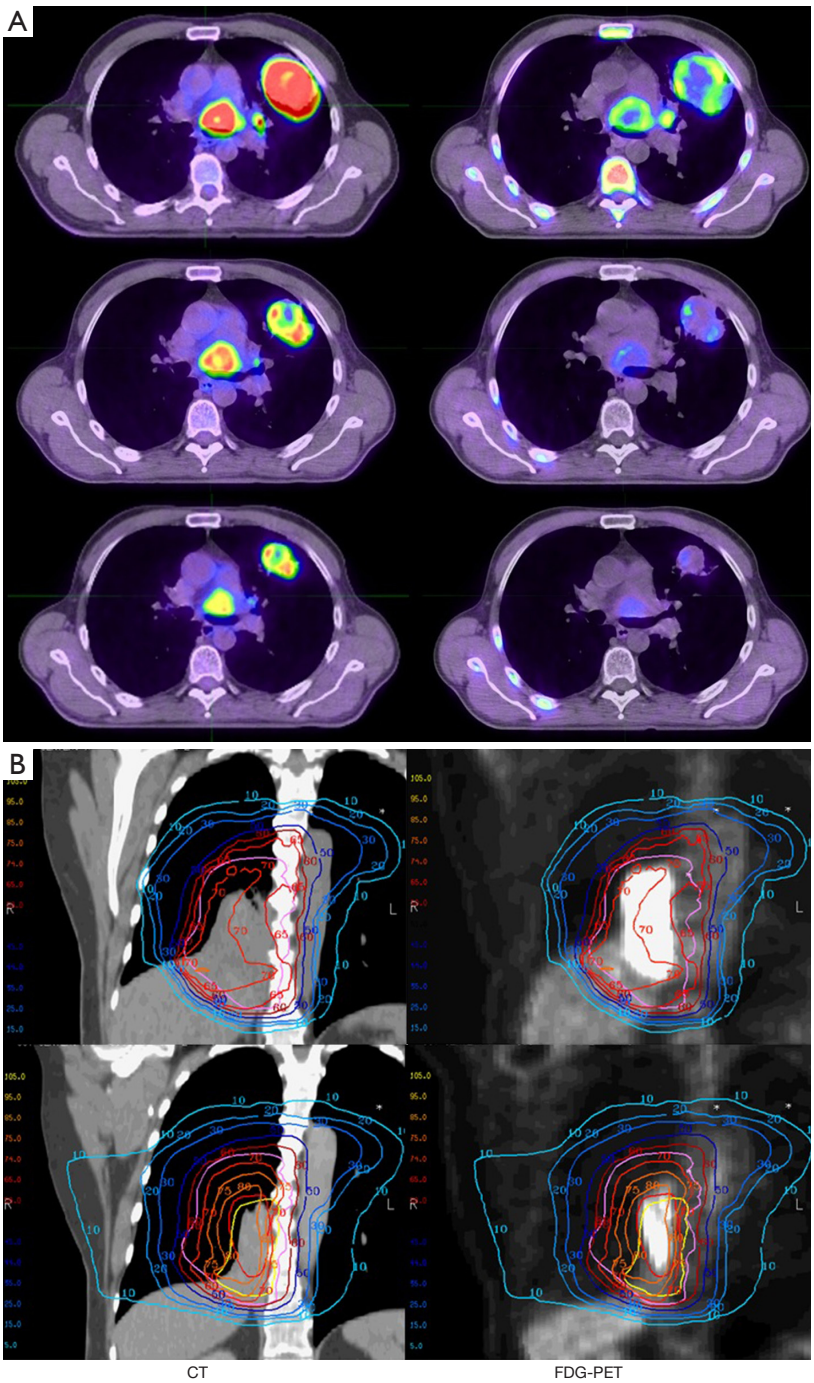

Figure 4 Response assessment with PET during therapy. (A) This patient with Stage IIIA NSCLC underwent serial FDG and FLT PET/CT scans prior to and during chemo-radiation therapy comprising baseline (top row), week 2 (middle row) and week 4 (bottom row), with FDG scans (left column) and FLT scans (right column). The FLT scans showed a more rapid and marked therapeutic response and complete disappearance of the bone marrow signal by week 2; (B) this patient had an initial radiation treatment plan using the baseline FDG-PET and CT scans (upper panels) that would deliver 60–66 Gy to FDG-avid tumor with a lung NTCP of 17.2%. Based on interim PET/CT, an adaptive plan was created that delivered 76–80 Gy to residual active tumor whilst maintaining a lung NTCP of 17.2%. PET, positron emission tomography; NSCLC, non-small cell lung cancer; FDG, ^{18}F-fluoro-deoxyglucose; CT, computed tomography; FLT, ^{18}F-fluorothymidine; NTCP, normal tissue complication probability.

dose escalation of 30–102 Gy (mean, 58 Gy) or a reduction in normal tissue complication probability (NTCP) of 0.4–3% (mean, 2%) in 5 of 6 patients with smaller yet residual tumor volumes (87). Following this study a phase II trial assessing the feasibility of PET guided adaptive treatment was conducted at University of Michigan (88). Adaptive planning used FDG-PET to measure tumor response after 50 Gy and the RT plan was adapted to target the residual metabolic target volume (MTV) for the final 9 fractions. Using an iso-toxic approach for a 17% risk of grade 3 RILT estimated from a mean lung dose NTCP model, the dose per fraction to the MTV based PTV varied from 2.2–3.8 Gy for the adaptive course of treatment. The 2-year rates of in-field LRTC and overall LRTC were 84% and 68% respectively (88).

RTOG 1106 is a current phase II clinical trial for patients with locally advanced NSCLC designed to determine whether slow-responding tumors can be dose-escalated to improve the local-regional progression-free rate at 2 years. FDG-PET/CT is used to measure the tumor response after 18–19 treatments and the final 9 treatments are adjusted to cover residual metabolic tumor volume. The adapted RT plan will be dose escalated up to 80.4 Gy to the MTV limiting dose according to an individualized MLD to 20 Gy and by esophageal and heart tolerance doses. Another appealing strategy would be to use during-treatment images as a biomarker to detect more radiosensitive tumors that require lower and less toxic doses for local control.

Imaging for treatment response assessment after completion of therapy

Cancer treatment response can be assessed by a range of imaging modalities and accordingly a range of different response criteria have evolved. The Response Evaluation Criteria in Solid Tumors (RECIST) was developed in 2000 (RECIST 1.0) was largely based on CT alone (89) and update in 2009 (RECIST 1.1) (90) included PET-CT for lung cancer. RECIST 1.1 is the most widely adopted system and represents the current standard for structural assessment of tumor response using CT or MRI. Target lesions (up to 2 per organ and 5 total are identified and the sum of the longest diameter (LD) of each target lesion is recorded. A complete response (CR) is defined as the disappearance of all target lesions, a partial response (PR) as at least a 30% decrease in the sum of the LD of target lesions, progressive disease (PD) as at least a 20% increase in the sum of the LD of target lesions or the appearance of new lesions, and SD as all other scenarios. There are several changes between RECIST 1.0 and RECIST 1.1. Previously, RECIST 1.0 required documentation of up to 10 target lesions (5 per organ)—now only 5 lesions (2 per organ) are required. RECIST 1.1 now includes size criteria for lymph nodes. Lymph nodes less than 10 mm short-axis diameter are considered non-pathological, between 10 and 15 mm they are considered non-target lesions, and ≥15 mm short axis are considered target lesions. There now also is a minimum absolute increase of 5 mm in lesions in addition to the 20% increase requirement to call PD.

Anatomical/structural imaging response assessment has significant limitations after RT for NSCLC. The presence of atelectasis or pneumonitis obscures tumor margins when assessing treatment response on CT and CT cannot detect tumor in small residual lymph nodes. The Peter MacCallum group in Australia, conducted prospective studies comparing FDG-PET and CT and reported that FGD-PET response was superior to CT for predicting survival (67) and was more strongly associated with patterns of failure (91). Patients with complete metabolic responses had excellent survival. The visual metabolic response criteria developed by this group have been widely adopted but in an effort to standardize methodology and ensure reproducibility, semiquantitative criteria have been developed.

Several systems are available to assess the treatment response using PET. In the PERCIST system (92), a fixed region of interest of about 1 cc in the most active region of a tumor is selected and SUV lean measurements are used as a continuous variable. A treatment response is defined as a 30% decline in SUV. The EORTC has also developed guidelines for response assessment using PET. EORTC criteria are based on adding max SUV from up to seven target lesions from as many organs as possible. Partial metabolic response (PMR) is defined as a reduction of the sum of max SUV of at least 25% and progressive metabolic disease (PMD) as an increase of the sum of max SUV of at least 25%. A comparison of response assessments using EORTC and PERCIST criteria suggests that both give similar responses and the association of metabolic response with overall survival is also similar between both criteria (93). Other assessment methods such as the Peter MacCallum and University of Michigan methods of assessment have also been evaluated in comparison to semiquantitative

assessment methods (94). The study of Wang (Kong) *et al.* reported that the PM visual method identified significantly more CMR cases than the 30% cutoff of semiquantitative assessment method from the University of Michigan (38.6% *vs.* 13.6%) (94). All of these methods can predict long term survival after therapy but a blinded head-to-head comparison of these methodologies is needed to determine which approach represents the best combination of predictive power, reproducibility and ease of use after RT for NSCLC.

Response assessment and detection of recurrent disease is especially difficult after SBRT and a range of criteria were initially suggested as indicative of recurrence (95). However, pseudotumors and other confounding changes are common in the months after treatment and many findings once regarded as indicating relapse are now regarded with more circumspection. Of the following CT imaging features that were initially considered signs of relapse: (I) opacity with new bulging margin; (II) opacification of air bronchograms; (III) enlarging pleural effusion; (IV) new or enlarging mass; and (V) increased lung density at the treatment site. A study of 218 early stage NSCLC patients treated with SABR only "new bulging margin at the treatment site" was strongly associated with local recurrence (96). In these challenging cases, metabolic imaging using FDG PET can often help differentiate between recurrence and post-treatment changes (97).

Radiomics is an emerging field with significant potential both for prognostic stratification based on baseline imaging studies and for response assessment in patients with lung cancer. Radiomics involves the extraction of additional quantitative data from medical images using advanced imaging processing and analysis tools (98). These quantitative data extend beyond what is visible to the human eye and can be powerfully correlated with patient outcomes (99,100). The use of radiomics for lung cancer is an active area of study (101-103). For example, Van Timmeren and colleagues have shown that radiomic features of CBCT images are associated with survival after RT in NSCLC (104).

Imaging of organs at risk during treatment

RT can cause early and late changes in normal tissues that can be detected by a range of imaging modalities including MRI, CT, PET, and SPECT. Late toxicities are more often seen because imaging has historically been used more in the post-radiation setting rather than during RT. Detection of early changes of toxicity during RT, at a time when therapy can be changed or toxicity treated pre-emptively, could potentially be very useful but is experimental at present. Organs at risk for RT toxicity include lungs, heart and esophagus. CT density in irradiated lung is correlated with cough and shortness of breath and other manifestation of radiation pneumonitis (105,106). MRI has also been shown to detect radiation pneumonitis by measuring lung density (107) and detecting unbalanced enhancement of the lung (108).

FDG uptake in pulmonary tissue detected on PET is associated with symptoms and signs of pneumonitis and PET changes may precede symptoms (77). Esophageal toxicities have been detected via PET scans when FDG uptake was detected in the esophagus during (109) and following radiation treatment (77,110-115) (*Figure 5A*). A study of 36 esophageal cancer patients identified a very congruent linear regression model connecting lung radiation dose and SUV changes (111). The effects of radiation on both lung and heart perfusion and lung ventilation have been assessed with SPECT (106,116,117). Sensitive assessments of lung perfusion with GalliPET indicate that significantly reduced perfusion may occur within the radiation volume early during RT (*Figure 5B*) (118). Cardiac disease may also impact upon decision making in lung cancer patients and, cardiac SPECT can be helpful in visualizing alterations in cardiac perfusion after RT (119-121).

Conclusions

The role of imaging in the management of lung cancer patients who are managed with RT is fundamental. Without advances in our ability to visualize and characterize tumors accurately, the rapid advances in accurate radiation treatment delivery in recent years would have been futile. Imaging plays a key role in every part of the patient journey, from screening, through diagnosis, staging selection for therapy, treatment planning, response assessment and early detection of recurrence should it occur. Future advances in imaging platforms and the development of new tracers will allow ever more detailed assessments of individual cancers to be made. The integration of more accurate and more personalized imaging with advances in tumor biological characterization, for example by the use of liquid biopsies employing circulating tumor cells (122) or circulating tumor DNA (123) have the potential to further improve the survival of patients with lung cancer treated with RT.

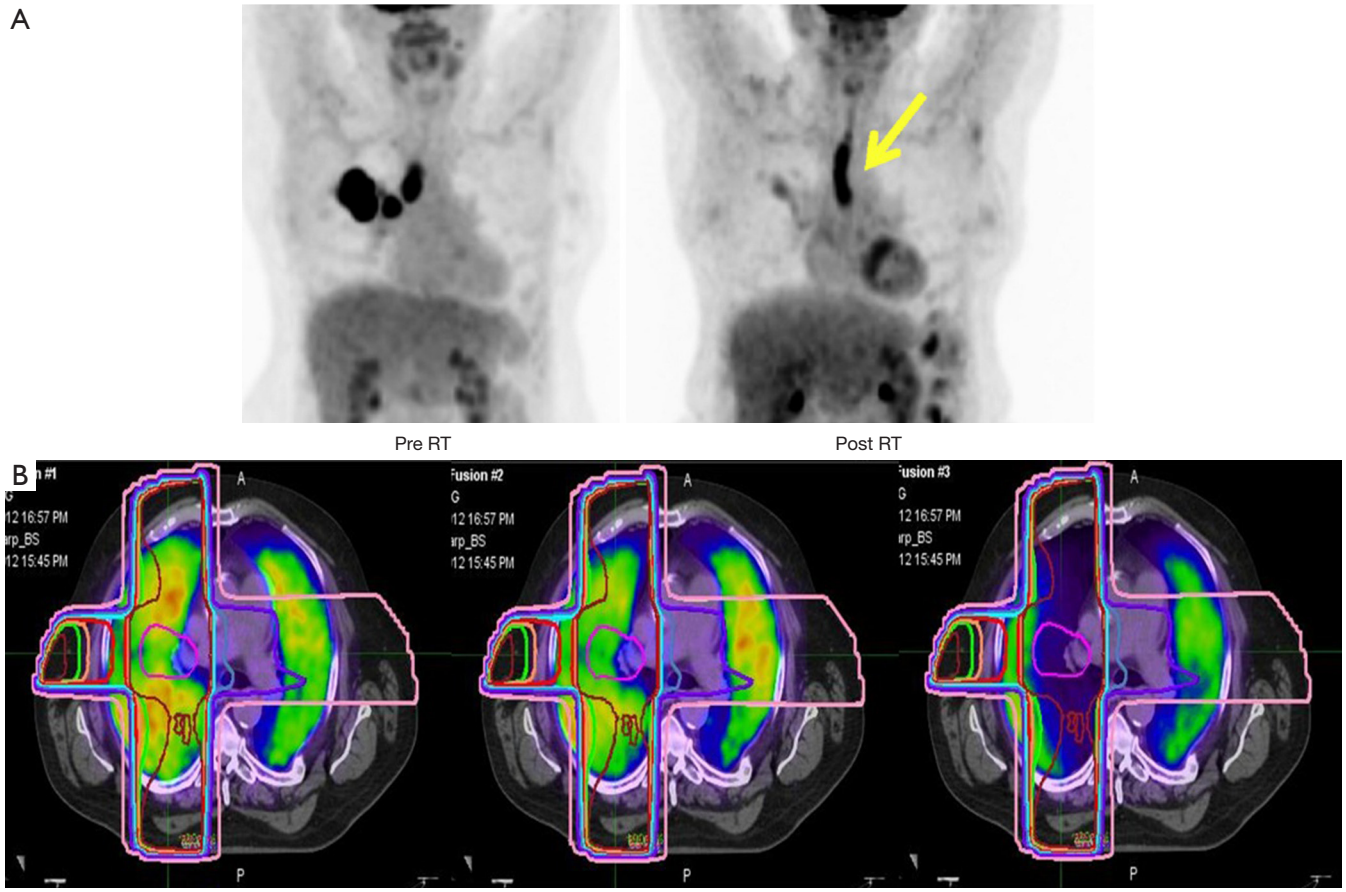

Figure 5 Imaging the normal tissue effects of radiation. (A) This patient with stage IIIA adenocarcinoma of the right upper lobe was treated with concomitant chemoRT to 62 Gy. Post treatment PET/CT showed both an excellent therapeutic response and increased FDG uptake in the esophagus. Esophagoscopy revealed ulceration and early stenosis. Yellow arrow indicates linear FDG uptake in the esophagus; (B) serial perfusion imaging with ^{68}Ga PET/CT in a patient treated with 60 Gy of external beam RT. By the mid-point of treatment a substantial reduction of blood flow had occurred in the high-dose volume. The post treatment scan shows extremely poor perfusion in the high-dose volume. PET, positron emission tomography; CT, computed tomography; FDG, ^{18}F-fluoro-deoxyglucose.

Acknowledgements

We are grateful to Dr. Shankar Siva for permission to use the Gallipet images in *Figure 5B*.

Footnote

Conflicts of Interest: The authors have no conflicts of interest to declare.

References

1. Akhurst T, MacManus M, Hicks RJ. Lung cancer. PET Clin 2015;10:147-58.
2. Dingemans AM, de Langen AJ, van den Boogaart V, et al. First-line erlotinib and bevacizumab in patients with locally advanced and/or metastatic non-small-cell lung cancer: a phase II study including molecular imaging. Ann Oncol 2011;22:559-66.
3. Murray P, Franks K, Hanna GG. A systematic review of outcomes following stereotactic ablative radiotherapy in the treatment of early-stage primary lung cancer. Br J Radiol 2017;90:20160732.
4. Steinfort DP, Siva S, Leong TL, et al. Systematic Endobronchial Ultrasound-guided Mediastinal Staging Versus Positron Emission Tomography for Comprehensive

Mediastinal Staging in NSCLC Before Radical Radiotherapy of Non-small Cell Lung Cancer: A Pilot Study. Medicine (Baltimore) 2016;95:e2488.
5. Chang JH, Gandhidasan S, Finnigan R, et al. Stereotactic Ablative Body Radiotherapy for the Treatment of Spinal Oligometastases. Clin Oncol (R Coll Radiol) 2017;29:e119-25.
6. Siva S, Senan S, Ball D. Ablative therapies for lung metastases: a need to acknowledge the efficacy and toxicity of stereotactic ablative body radiotherapy. Ann Oncol 2015;26:2196.
7. Gomez DR, Blumenschein GR Jr, Lee JJ, et al. Local consolidative therapy versus maintenance therapy or observation for patients with oligometastatic non-small-cell lung cancer without progression after first-line systemic therapy: a multicentre, randomised, controlled, phase 2 study. Lancet Oncol 2016;17:1672-82.
8. Sulman EP, Komaki R, Klopp AH, et al. Exclusion of elective nodal irradiation is associated with minimal elective nodal failure in non-small cell lung cancer. Radiat Oncol 2009;4:5.
9. Siva S, Callahan J, MacManus MP, et al. Abscopal [corrected] effects after conventional and stereotactic lung irradiation of non-small-cell lung cancer. J Thorac Oncol 2013;8:e71-2.
10. Goldstraw P, Chansky K, Crowley J, et al. The IASLC Lung Cancer Staging Project: Proposals for Revision of the TNM Stage Groupings in the Forthcoming (Eighth) Edition of the TNM Classification for Lung Cancer. J Thorac Oncol 2016;11:39-51.
11. Glazer GM, Orringer MB, Gross BH, et al. The mediastinum in non-small cell lung cancer: CT-surgical correlation. AJR Am J Roentgenol 1984;142:1101-5.
12. Andersen MB, Harders SW, Ganeshan B, et al. CT texture analysis can help differentiate between malignant and benign lymph nodes in the mediastinum in patients suspected for lung cancer. Acta Radiol 2016;57:669-76.
13. Metcalfe P, Liney GP, Holloway L, et al. The potential for an enhanced role for MRI in radiation-therapy treatment planning. Technol Cancer Res Treat 2013;12:429-46.
14. Yun M, Kim W, Alnafisi N, et al. 18F-FDG PET in characterizing adrenal lesions detected on CT or MRI. J Nucl Med 2001;42:1795-9.
15. Seute T, Leffers P, ten Velde GP, et al. Detection of brain metastases from small cell lung cancer: consequences of changing imaging techniques (CT versus MRI). Cancer 2008;112:1827-34.
16. Hjorthaug K, Hojbjerg JA, Knap MM, et al. Accuracy of 18F-FDG PET-CT in triaging lung cancer patients with suspected brain metastases for MRI. Nucl Med Commun 2015;36:1084-90.
17. Yuan ST, Frey KA, Gross MD, et al. Semiquantification and classification of local pulmonary function by V/Q single photon emission computed tomography in patients with non-small cell lung cancer: potential indication for radiotherapy planning. J Thorac Oncol 2011;6:71-8.
18. Meng X, Frey K, Matuszak M, et al. Changes in functional lung regions during the course of radiation therapy and their potential impact on lung dosimetry for non-small cell lung cancer. Int J Radiat Oncol Biol Phys 2014;89:145-51.
19. Callahan J, Hofman MS, Siva S, et al. High-resolution imaging of pulmonary ventilation and perfusion with 68Ga-VQ respiratory gated (4-D) PET/CT. Eur J Nucl Med Mol Imaging 2014;41:343-9.
20. Siva S, Devereux T, Ball DL, et al. Ga-68 MAA Perfusion 4D-PET/CT Scanning Allows for Functional Lung Avoidance Using Conformal Radiation Therapy Planning. Technol Cancer Res Treat 2016;15:114-21.
21. Herder GJ, Golding RP, Hoekstra OS, et al. The performance of(18)F-fluorodeoxyglucose positron emission tomography in small solitary pulmonary nodules. Eur J Nucl Med Mol Imaging 2004;31:1231-6.
22. Søgaard R, Fischer BM, Mortensen J, et al. Preoperative staging of lung cancer with PET/CT: cost-effectiveness evaluation alongside a randomized controlled trial. Eur J Nucl Med Mol Imaging 2011;38:802-9.
23. Videtic GM, Rice TW, Murthy S, et al. Utility of positron emission tomography compared with mediastinoscopy for delineating involved lymph nodes in stage III lung cancer: insights for radiotherapy planning from a surgical cohort. Int J Radiat Oncol Biol Phys 2008;72:702-6.
24. Steinfort DP, Liew D, Irving LB. Radial probe EBUS versus CT-guided needle biopsy for evaluation of peripheral pulmonary lesions: an economic analysis. Eur Respir J 2013;41:539-47.
25. Bury T, Barreto A, Daenen F, et al. Fluorine-18 deoxyglucose positron emission tomography for the detection of bone metastases in patients with non-small cell lung cancer. Eur J Nucl Med 1998;25:1244-7.
26. MacManus MP, Hicks RJ, Matthews JP, et al. High rate of detection of unsuspected distant metastases by pet in apparent stage III non-small-cell lung cancer: implications for radical radiation therapy. Int J Radiat Oncol Biol Phys 2001;50:287-93.

27. Ball D, Everitt S, Hicks R, et al. Serial FDG and FLT PET/CT during Curative-Intent Chemo-Radiotherapy for NSCLC Impacts Patient Management and May Predict Clinical Outcomes. J Thorac Oncol 2017;12:S420.
28. Mac Manus MP, Wong K, Hicks RJ, et al. Early mortality after radical radiotherapy for non-small-cell lung cancer: comparison of PET-staged and conventionally staged cohorts treated at a large tertiary referral center. Int J Radiat Oncol Biol Phys 2002;52:351-61.
29. Mac Manus MP, Hicks RJ, Ball DL, et al. F-18 fluorodeoxyglucose positron emission tomography staging in radical radiotherapy candidates with nonsmall cell lung carcinoma: powerful correlation with survival and high impact on treatment. Cancer 2001;92:886-95.
30. Mac Manus MP, Everitt S, Bayne M, et al. The use of fused PET/CT images for patient selection and radical radiotherapy target volume definition in patients with non-small cell lung cancer: results of a prospective study with mature survival data. Radiother Oncol 2013;106:292-8.
31. Geiger GA, Kim MB, Xanthopoulos EP, et al. Stage migration in planning PET/CT scans in patients due to receive radiotherapy for non-small-cell lung cancer. Clin Lung Cancer 2014;15:79-85.
32. Everitt S, Herschtal A, Callahan J, et al. High rates of tumor growth and disease progression detected on serial pretreatment fluorodeoxyglucose-positron emission tomography/computed tomography scans in radical radiotherapy candidates with nonsmall cell lung cancer. Cancer 2010;116:5030-7.
33. Wang J, Mahasittiwat P, Wong KK, et al. Natural growth and disease progression of non-small cell lung cancer evaluated with 18F-fluorodeoxyglucose PET/CT. Lung Cancer 2012;78:51-6.
34. Everitt S, Plumridge N, Herschtal A, et al. The impact of time between staging PET/CT and definitive chemo-radiation on target volumes and survival in patients with non-small cell lung cancer. Radiother Oncol 2013;106:288-91.
35. Konert T, Vogel W, MacManus MP, et al. PET/CT imaging for target volume delineation in curative intent radiotherapy of non-small cell lung cancer: IAEA consensus report 2014. Radiother Oncol 2015;116:27-34.
36. Nestle U, Walter K, Schmidt S, et al. 18F-deoxyglucose positron emission tomography (FDG-PET) for the planning of radiotherapy in lung cancer: high impact in patients with atelectasis. Int J Radiat Oncol Biol Phys 1999;44:593-7.
37. De Ruysscher D, Wanders S, van Haren E, et al. Selective mediastinal node irradiation based on FDG-PET scan data in patients with non-small-cell lung cancer: a prospective clinical study. Int J Radiat Oncol Biol Phys 2005;62:988-94.
38. Caldwell CB, Mah K, Ung YC, et al. Observer variation in contouring gross tumor volume in patients with poorly defined non-small-cell lung tumors on CT: the impact of 18FDG-hybrid PET fusion. Int J Radiat Oncol Biol Phys 2001;51:923-31.
39. Werner-Wasik M, Nelson AD, Choi W, et al. What is the best way to contour lung tumors on PET scans? Multiobserver validation of a gradient-based method using a NSCLC digital PET phantom. Int J Radiat Oncol Biol Phys 2012;82:1164-71.
40. Hatt M, Lee JA, Schmidtlein CR, et al. Classification and evaluation strategies of auto-segmentation approaches for PET: Report of AAPM task group No. 211. Med Phys 2017;44:e1-42.
41. MacManus M, Nestle U, Rosenzweig KE, et al. Use of PET and PET/CT for radiation therapy planning: IAEA expert report 2006-2007. Radiother Oncol 2009;91:85-94.
42. Doll C, Duncker-Rohr V, Rucker G, et al. Influence of experience and qualification on PET-based target volume delineation. When there is no expert--ask your colleague. Strahlenther Onkol 2014;190:555-62.
43. Mahasittiwat P, Yuan S, Xie C, et al. Metabolic Tumor Volume on PET Reduced More than Gross Tumor Volume on CT during Radiotherapy in Patients with Non-Small Cell Lung Cancer Treated with 3DCRT or SBRT. J Radiat Oncol 2013;2:191-202.
44. Wielpütz M, Kauczor HU. MRI of the lung: state of the art. Diagn Interv Radiol 2012;18:344-53.
45. Silvestri GA, Gonzalez AV, Jantz MA, et al. Methods for staging non-small cell lung cancer: Diagnosis and management of lung cancer, 3rd ed: American College of Chest Physicians evidence-based clinical practice guidelines. Chest 2013;143:e211S-50S.
46. Brandner ED, Chetty IJ, Giaddui TG, et al. Motion management strategies and technical issues associated with stereotactic body radiotherapy of thoracic and upper abdominal tumors: A review from NRG oncology. Med Phys 2017;44:2595-612.
47. De Ruysscher D, Faivre-Finn C, Nestle U, et al. European Organisation for Research and Treatment of Cancer recommendations for planning and delivery of high-dose, high-precision radiotherapy for lung cancer. J Clin Oncol 2010;28:5301-10.

48. Chirindel A, Adebahr S, Schuster D, et al. Impact of 4D-(18)FDG-PET/CT imaging on target volume delineation in SBRT patients with central versus peripheral lung tumors. Multi-reader comparative study. Radiother Oncol 2015;115:335-41.
49. Callahan J, Kron T, Siva S, et al. Geographic miss of lung tumours due to respiratory motion: a comparison of 3D vs 4D PET/CT defined target volumes. Radiat Oncol 2014;9:291.
50. Sindoni A, Minutoli F, Pontoriero A, et al. Usefulness of four dimensional (4D) PET/CT imaging in the evaluation of thoracic lesions and in radiotherapy planning: Review of the literature. Lung Cancer 2016;96:78-86.
51. Adebahr S, Collette S, Shash E, et al. LungTech, an EORTC Phase II trial of stereotactic body radiotherapy for centrally located lung tumours: a clinical perspective. Br J Radiol 2015;88:20150036.
52. Lambrecht M, Melidis C, Sonke JJ, et al. Lungtech, a phase II EORTC trial of SBRT for centrally located lung tumours - a clinical physics perspective. Radiat Oncol 2016;11:7.
53. De Ruysscher D, Wanders S, Minken A, et al. Effects of radiotherapy planning with a dedicated combined PET-CT-simulator of patients with non-small cell lung cancer on dose limiting normal tissues and radiation dose-escalation: a planning study. Radiother Oncol 2005;77:5-10.
54. Fleckenstein J, Hellwig D, Kremp S, et al. F-18-FDG-PET confined radiotherapy of locally advanced NSCLC with concomitant chemotherapy: results of the PET-PLAN pilot trial. Int J Radiat Oncol Biol Phys 2011;81:e283-9.
55. Nestle U, Rischke HC, Eschmann SM, et al. Improved inter-observer agreement of an expert review panel in an oncology treatment trial--Insights from a structured interventional process. Eur J Cancer 2015;51:2525-33.
56. van Elmpt W, De Ruysscher D, van der Salm A, et al. The PET-boost randomised phase II dose-escalation trial in non-small cell lung cancer. Radiother Oncol 2012;104:67-71.
57. Even AJ, van der Stoep J, Zegers CM, et al. PET-based dose painting in non-small cell lung cancer: Comparing uniform dose escalation with boosting hypoxic and metabolically active sub-volumes. Radiother Oncol 2015;116:281-6.
58. Ruschin M, Sahgal A, Tseng CL, et al. Dosimetric Impact of Using a Virtual Couch Shift for Online Correction of Setup Errors for Brain Patients on an Integrated High-Field Magnetic Resonance Imaging Linear Accelerator. Int J Radiat Oncol Biol Phys 2017;98:699-708.
59. Erridge SC, Seppenwoolde Y, Muller SH, et al. Portal imaging to assess set-up errors, tumor motion and tumor shrinkage during conformal radiotherapy of non-small cell lung cancer. Radiother Oncol 2003;66:75-85.
60. Michienzi A, Kron T, Callahan J, et al. Cone-beam computed tomography for lung cancer - validation with CT and monitoring tumour response during chemo-radiation therapy. J Med Imaging Radiat Oncol 2017;61:263-70.
61. Lim G, Bezjak A, Higgins J, et al. Tumor Regression and Positional Changes in Non-small Cell Lung Cancer During Radical Radiotherapy. J Thorac Oncol 2011;6:531-6.
62. Kupelian PA, Ramsey C, Meeks SL, et al. Serial megavoltage CT imaging during external beam radiotherapy for non-small-cell lung cancer: observations on tumor regression during treatment. Int J Radiat Oncol Biol Phys 2005;63:1024-8.
63. van Zwienen M, van Beek S, Belderbos J, et al. Anatomical Changes during Radiotherapy of Lung Cancer Patients. Int J Radiat Oncol Biol Phys 2008;72.
64. Koo TR, Moon SH, Lim YJ, et al. The effect of tumor volume and its change on survival in stage III non-small cell lung cancer treated with definitive concurrent chemoradiotherapy. Radiat Oncol 2014;9:283.
65. Paul J, Yang C, Wu H, et al. Early Assessment of Treatment Responses During Radiation Therapy for Lung Cancer Using Quantitative Analysis of Daily Computed Tomography. Int J Radiat Oncol Biol Phys 2017;98:463-72.
66. Lee J, Lee J, Choi J, et al. Early treatment volume reduction rate as a prognostic factor in patients treated with chemoradiotherapy for limited stage small cell lung cancer. Radiat Oncol J 2015;33:117-25.
67. Mac Manus MP, Hicks RJ, Matthews JP, et al. Positron emission tomography is superior to computed tomography scanning for response-assessment after radical radiotherapy or chemoradiotherapy in patients with non-small-cell lung cancer. J Clin Oncol 2003;21:1285-92.
68. Jaffray DA, Siewerdsen JH, Wong JW, et al. Flat-panel cone-beam computed tomography for image-guided radiation therapy. Int J Radiat Oncol Biol Phys 2002;53:1337-49.
69. Nielsen M, Bertelsen A, Westberg J, et al. Cone beam CT evaluation of patient set-up accuracy as a QA tool. Acta Oncologica 2009;48:271-6.
70. Jaffray DA, Drake DG, Moreau M, et al. A radiographic and tomographic imaging system integrated into a medical

linear accelerator for localization of bone and soft-tissue targets. Int J Radiat Oncol Biol Phys 1999;45:773-89.
71. Sorcini B, Tilikidis A. Clinical application of image-guided radiotherapy, IGRT (on the Varian OBI platform). Cancer Radiother 2006;10:252-7.
72. Kong FM, Frey KA, Quint LE, et al. A pilot study of [18F] fluorodeoxyglucose positron emission tomography scans during and after radiation-based therapy in patients with non small-cell lung cancer. J Clin Oncol 2007;25:3116-23.
73. Harris JP, Chang-Halpenny CN, Maxim PG, et al. Outcomes of Modestly Hypofractionated Radiation for Lung Tumors: Pre- and Mid-Treatment Positron Emission Tomography-Computed Tomography Metrics as Prognostic Factors. Clin Lung Cancer 2015;16:475-85.
74. Massaccesi M, Calcagni ML, Spitilli MG, et al. (1)(8) F-FDG PET-CT during chemo-radiotherapy in patients with non-small cell lung cancer: the early metabolic response correlates with the delivered radiation dose. Radiat Oncol 2012;7:106.
75. van Baardwijk A, Bosmans G, Dekker A, et al. Time trends in the maximal uptake of FDG on PET scan during thoracic radiotherapy. A prospective study in locally advanced non-small cell lung cancer (NSCLC) patients. Radiother Oncol 2007;82:145-52.
76. Bollineni VR, Widder J, Pruim J, et al. Residual (1)(8) F-FDG-PET uptake 12 weeks after stereotactic ablative radiotherapy for stage I non-small-cell lung cancer predicts local control. Int J Radiat Oncol Biol Phys 2012;83:e551-5.
77. Mac Manus MP, Ding Z, Hogg A, et al. Association between pulmonary uptake of fluorodeoxyglucose detected by positron emission tomography scanning after radiation therapy for non-small-cell lung cancer and radiation pneumonitis. Int J Radiat Oncol Biol Phys 2011;80:1365-71.
78. Everitt SJ, Ball DL, Hicks RJ, et al. Differential (18)F-FDG and (18)F-FLT Uptake on Serial PET/CT Imaging Before and During Definitive Chemoradiation for Non-Small Cell Lung Cancer. J Nucl Med 2014;55:1069-74.
79. Bollineni VR, Wiegman EM, Pruim J, et al. Hypoxia imaging using Positron Emission Tomography in non-small cell lung cancer: implications for radiotherapy. Cancer Treat Rev 2012;38:1027-32.
80. Bollineni VR, Kerner GS, Pruim J, et al. PET imaging of tumor hypoxia using 18F-fluoroazomycin arabinoside in stage III-IV non-small cell lung cancer patients. J Nucl Med 2013;54:1175-80.
81. Vera P, Bohn P, Edet-Sanson A, et al. Simultaneous positron emission tomography (PET) assessment of metabolism with (1)(8)F-fluoro-2-deoxy-d-glucose (FDG), proliferation with (1)(8)F-fluoro-thymidine (FLT), and hypoxia with (1)(8)fluoro-misonidazole (F-miso) before and during radiotherapy in patients with non-small-cell lung cancer (NSCLC): a pilot study. Radiother Oncol 2011;98:109-16.
82. Koh WJ, Bergman KS, Rasey JS, et al. Evaluation of oxygenation status during fractionated radiotherapy in human nonsmall cell lung cancers using [F-18] fluoromisonidazole positron emission tomography. Int J Radiat Oncol Biol Phys 1995;33:391-8.
83. Trinkaus ME, Blum R, Rischin D, et al. Imaging of hypoxia with (18) F-FAZA PET in patients with locally advanced non-small cell lung cancer treated with definitive chemoradiotherapy. J Med Imaging Radiat Oncol 2013;57:475-81.
84. Yan D, Lockman D, Martinez A, et al. Computed tomography guided management of interfractional patient variation. Semin Radiat Oncol 2005;15:168-79.
85. Li XA, Qi XS, Pitterle M, et al. Interfractional variations in patient setup and anatomic change assessed by daily computed tomography. Int J Radiat Oncol Biol Phys 2007;68:581-91.
86. Hugo GD, Yan D, Liang J. Population and patient-specific target margins for 4D adaptive radiotherapy to account for intra- and inter-fraction variation in lung tumour position. Phys Med Biol 2007;52:257-74.
87. Feng M, Kong FM, Gross M, et al. Using fluorodeoxyglucose positron emission tomography to assess tumor volume during radiotherapy for non-small-cell lung cancer and its potential impact on adaptive dose escalation and normal tissue sparing. Int J Radiat Oncol Biol Phys 2009;73:1228-34.
88. Kong F, Ten Haken RK, Schipper MJ, et al. A phase II trial of mid-treatment FDG-PET adaptive, individualized radiation therapy plus concurrent chemotherapy in patients with non-small cell lung cancer (NSCLC). J Clin Oncol 2013;31 suppl:abstr 7522.
89. Therasse P, Arbuck SG, Eisenhauer EA, et al. New guidelines to evaluate the response to treatment in solid tumors. European Organization for Research and Treatment of Cancer, National Cancer Institute of the United States, National Cancer Institute of Canada. J Natl Cancer Inst 2000;92:205-16.
90. Eisenhauer EA, Therasse P, Bogaerts J, et al. New response evaluation criteria in solid tumours: revised RECIST

guideline (version 1.1). Eur J Cancer 2009;45:228-47.
91. Mac Manus MP, Hicks RJ, Matthews JP, et al. Metabolic (FDG-PET) response after radical radiotherapy/chemoradiotherapy for non-small cell lung cancer correlates with patterns of failure. Lung Cancer 2005;49:95-108.
92. Wahl RL, Jacene H, Kasamon Y, et al. From RECIST to PERCIST: Evolving Considerations for PET response criteria in solid tumors. J Nucl Med 2009;50 Suppl 1:122S-50S.
93. Skougaard K, Nielsen D, Jensen BV, et al. Comparison of EORTC criteria and PERCIST for PET/CT response evaluation of patients with metastatic colorectal cancer treated with irinotecan and cetuximab. J Nucl Med 2013;54:1026-31.
94. Wang J, Wong KK, Piert M, et al. Metabolic response assessment with F-FDG PET/CT: inter-method comparison and prognostic significance for patients with non-small cell lung cancer. J Radiat Oncol 2015;4:249-56.
95. Huang K, Senthi S, Palma DA, et al. High-risk CT features for detection of local recurrence after stereotactic ablative radiotherapy for lung cancer. Radiother Oncol 2013;109:51-7.
96. Halpenny D, Ridge CA, Hayes S, et al. Computed tomographic features predictive of local recurrence in patients with early stage lung cancer treated with stereotactic body radiation therapy. Clin Imaging 2015;39:254-8.
97. Juweid ME, Cheson BD. Positron-emission tomography and assessment of cancer therapy. N Engl J Med 2006;354:496-507.
98. Leijenaar RT, Carvalho S, Hoebers FJ, et al. External validation of a prognostic CT-based radiomic signature in oropharyngeal squamous cell carcinoma. Acta Oncol 2015;54:1423-9.
99. Lambin P, Rios-Velazquez E, Leijenaar R, et al. Radiomics: extracting more information from medical images using advanced feature analysis. Eur J Cancer 2012;48:441-6.
100. Huynh E, Coroller TP, Narayan V, et al. Associations of Radiomic Data Extracted from Static and Respiratory-Gated CT Scans with Disease Recurrence in Lung Cancer Patients Treated with SBRT. PLoS One 2017;12:e0169172.
101. Parmar C, Leijenaar RT, Grossmann P, et al. Radiomic feature clusters and prognostic signatures specific for Lung and Head & Neck cancer. Sci Rep 2015;5:11044.
102. Coroller TP, Grossmann P, Hou Y, et al. CT-based radiomic signature predicts distant metastasis in lung adenocarcinoma. Radiother Oncol 2015;114:345-50.
103. Cunliffe A, Armato SG 3rd, Castillo R, et al. Lung texture in serial thoracic computed tomography scans: correlation of radiomics-based features with radiation therapy dose and radiation pneumonitis development. Int J Radiat Oncol Biol Phys 2015;91:1048-56.
104. van Timmeren JE, Leijenaar RTH, van Elmpt W, et al. Survival prediction of non-small cell lung cancer patients using radiomics analyses of cone-beam CT images. Radiother Oncol 2017;123:363-9.
105. Mah K, Van Dyk J, Keane T, et al. Acute radiation-induced pulmonary damage: a clinical study on the response to fractionated radiation therapy. Int J Radiat Oncol Biol Phys 1987;13:179-88.
106. Boersma LJ, Damen EM, de Boer RW, et al. Recovery of overall and local lung function loss 18 months after irradiation for malignant lymphoma. J Clin Oncol 1996;14:1431-41.
107. Yankelevitz DF, Henschke CI, Batata M, et al. Lung cancer: evaluation with MR imaging during and after irradiation. J Thorac Imaging 1994;9:41-6.
108. Ogasawara N, Suga K, Karino Y, et al. Perfusion characteristics of radiation-injured lung on Gd-DTPA-enhanced dynamic magnetic resonance imaging. Invest Radiol 2002;37:448-57.
109. Yuan ST, Brown RK, Zhao L, et al. Timing and intensity of changes in FDG uptake with symptomatic esophagitis during radiotherapy or chemo-radiotherapy. Radiat Oncol 2014;9:37.
110. Hicks RJ, Mac Manus MP, Matthews JP, et al. Early FDG-PET imaging after radical radiotherapy for non-small-cell lung cancer: inflammatory changes in normal tissues correlate with tumor response and do not confound therapeutic response evaluation. Int J Radiat Oncol Biol Phys 2004;60:412-8.
111. Guerrero T, Johnson V, Hart J, et al. Radiation pneumonitis: local dose versus [18F]-fluorodeoxyglucose uptake response in irradiated lung. Int J Radiat Oncol Biol Phys 2007;68:1030-5.
112. Hart JP, McCurdy MR, Ezhil M, et al. Radiation pneumonitis: correlation of toxicity with pulmonary metabolic radiation response. Int J Radiat Oncol Biol Phys 2008;71:967-71.
113. Abdulla S, Salavati A, Saboury B, et al. Quantitative assessment of global lung inflammation following radiation therapy using FDG PET/CT: a pilot study. Eur J Nucl Med Mol Imaging 2014;41:350-6.

114. McCurdy M, Bergsma DP, Hyun E, et al. The Role of Lung Lobes in Radiation Pneumonitis and Radiation-Induced Inflammation in the Lung: A Retrospective Study. J Radiat Oncol 2013;2:203-8.
115. McCurdy MR, Castillo R, Martinez J, et al. [18F]-FDG uptake dose-response correlates with radiation pneumonitis in lung cancer patients. Radiother Oncol 2012;104:52-7.
116. Seppenwoolde Y, De Jaeger K, Boersma LJ, et al. Regional differences in lung radiosensitivity after radiotherapy for non-small-cell lung cancer. Int J Radiat Oncol Biol Phys 2004;60:748-58.
117. Marks LB, Fan M, Clough R, et al. Radiation-induced pulmonary injury: symptomatic versus subclinical endpoints. Int J Radiat Biol 2000;76:469-75.
118. Siva S, Hardcastle N, Kron T, et al. Ventilation/Perfusion Positron Emission Tomography--Based Assessment of Radiation Injury to Lung. Int J Radiat Oncol Biol Phys 2015;93:408-17.
119. Maunoury C, Pierga JY, Valette H, et al. Myocardial perfusion damage after mediastinal irradiation for Hodgkin's disease: a thallium-201 single photon emission tomography study. Eur J Nucl Med 1992;19:871-3.
120. Prosnitz RG, Hubbs JL, Evans ES, et al. Prospective assessment of radiotherapy-associated cardiac toxicity in breast cancer patients: analysis of data 3 to 6 years after treatment. Cancer 2007;110:1840-50.
121. Zellars R, Bravo PE, Tryggestad E, et al. SPECT analysis of cardiac perfusion changes after whole-breast/chest wall radiation therapy with or without active breathing coordinator: results of a randomized phase 3 trial. Int J Radiat Oncol Biol Phys 2014;88:778-85.
122. Martin OA, Anderson RL, Russell PA, et al. Mobilization of viable tumor cells into the circulation during radiation therapy. Int J Radiat Oncol Biol Phys 2014;88:395-403.
123. Newman AM, Bratman SV, To J, et al. An ultrasensitive method for quantitating circulating tumor DNA with broad patient coverage. Nat Med 2014;20:548-54.

Cite this article as: MacManus M, Everitt S, Schimek-Jasch T, Li XA, Nestle U, Kong FM. Anatomic, functional and molecular imaging in lung cancer precision radiation therapy: treatment response assessment and radiation therapy personalization. Transl Lung Cancer Res 2017;6(6):670-688. doi: 10.21037/tlcr.2017.09.05

